

# Modelling, Simulation and Validation of Plastic Zone Size during Deformation of Mild Steel

S. O. Adeosun, E. I. Akpan, S. A. Balogun, O. O. Taiwo

**Abstract**—A model to predict the plastic zone size for material under plane stress condition has been developed and verified experimentally. The developed model is a function of crack size, crack angle and material property (dislocation density). Simulation and validation results show that the model developed show good agreement with experimental results. Samples of low carbon steel (0.035%C) with included surface crack angles of 45°, 50°, 60°, 70° and 90° and crack depths of 2mm and 4mm were subjected to low strain rate between  $0.48 \times 10^{-3} \text{ s}^{-1}$  –  $2.38 \times 10^{-3} \text{ s}^{-1}$ . The mechanical properties studied were ductility, tensile strength, modulus of elasticity, yield strength, yield strain, stress at fracture and fracture toughness. The experimental study shows that strain rate has no appreciable effect on the size of plastic zone while crack depth and crack angle plays an imperative role in determining the size of the plastic zone of mild steel materials.

**Keywords**—Applied stress, crack angle, crack size, material property, plastic zone size, strain rate.

## I. INTRODUCTION

PLASTIC zone size developed near the tip of a growing crack is regarded as a measure of material resistance against the crack driving force, the larger plastic zone size yields the higher toughness via the plastic energy dissipation [1]. Plastic region forms as a result of stress concentration at the tip of crack and it is a measure of the fracture toughness of the material [2]. This makes the study of crack-tip plastic zone size of fundamental importance in describing the process of failure from a macroscopic viewpoint and in formulating various fracture criteria.

Theoretically, linear elastic stress analysis of sharp cracks predicts infinite stresses at the crack tip. Inelastic deformation such as plasticity in metals and crazing in polymers, leads to relaxation of crack tip stresses caused by the yielding phenomenon at the crack tip. As a result, a plastic zone is formed containing micro structural defects such as dislocations and voids. Consequently, the local stresses are limited to the yield strength of the material. This implies that the elastic stress analysis becomes increasingly inaccurate as the inelastic region at the crack tip becomes sufficiently large and linear elastic fracture mechanics (LEFM) is no longer

O.O. Taiwo is with the Metallurgical and Materials Engineering Department, University of Lagos, Akoka, Nigeria (phone: +2348030432688; e-mail: taiwooluwaseyi2003@yahoo.com).

S.O. Adeosun and S.A Balogun are with the Metallurgical and Materials Engineering Department, University of Lagos, Akoka, (e-mail: sadeosun@unilag.edu.ng, sanmbo2003@yahoo.co.uk).

E.I Akpan is with the Metallurgical and Materials Engineering Department, Ambrose Alli University, Ekpoma, Nigeria. (e-mail: emma\_eia@yahoo.com).

useful for predicting the field equations [3].

Reference [4] has performed detailed analysis on the maximum stresses and the effects of several factors, e.g., the elastic mismatch have been explored. Kang and Kim [1] have shown that the unusual stress distribution is similar to the friction hill which occurs during plane strain compression [5]. Also, the magnitude of the maximum normal stress, which controls cavitation or brittle de-bonding, has been found to be proportional to the plastic zone size. Therefore, the fracture of the constrained ductile layer appears to be dependent on the plastic zone size, too.

Analytical methods have been limited to relatively simple crack related problems and various numerical analyses such as finite element method have been widely used and boundary element methods have been reported for example [2], [6]. Special approaches such as Dynamic Molecular Simulation [7], Orientation Gradient Mapping (OGM) and Electron Channeling Contrast Imaging (ECCI) [8] and computer simulation based on equaling Von Misses criteria (using Irwin's elastic solutions) to monotonic yield strength of material [9] has also been reported. However, these models are usually restricted to plates of infinite extent with simple geometrical configurations of crack and do not consider the combined influence of plate width, crack size and dislocation density on the plastic zone size.

For a homogeneous material under mode-I loading and small scale yielding condition, the well-known models by [10] and [11] have been used to predict the plastic zone size. In this work, a model different from that of Irwin have been proposed to predict the plastic zone size in a ductile mild steel and validated using experimental results.

## II. METHODOLOGY

### A. Theoretical Procedure

In deriving a model, dimensional analysis was made use of. Buckingham pi – method was used in other to determine the relative significance of each parameter affecting plastic zone size. Plastic zone size ( $r$ ) is a function of crack size ( $a$ ), crack angle ( $\theta$ ), applied stress ( $\sigma$ ), material property ( $N$ ) and strain rate ( $\dot{s}$ ).

Using Buckingham's method

$$r = f(a, \theta, \dot{s}, \sigma, N) \quad (1)$$

$$f_1(r, a, \theta, \dot{s}, \sigma, N) = 0 \quad (2)$$

Writing dimensions of each variable, where  $L$  = Length (metres),  $M$  = Mass (Kg),  $T$  = Time (s) we have

$$r = L, a = L, \theta = M^0 L^0 T^0, \dot{s} = T^{-1}, \sigma = ML^{-1}T^{-2}, N = L^{-2}$$

$$r = \phi(a^3 N \theta) \tag{9}$$

Thus, number of fundamental dimensions,  $m = 3$

$$\text{Number of } \pi\text{-terms} = n - m = 6 - 3 = 3$$

Equation (2) can be written as:

$$f_1(\pi_1, \pi_2, \pi_3) = 0 \tag{3}$$

Each  $\pi$ -terms contains  $(m + 1)$  variables, where  $m = 3$  and is also equal to repeating variables ( $r$  being a dependent variable should not be chosen as repeating variable), we get three  $\pi$ -terms as:

- $\pi_1 = (a, s, \sigma, r)$
- $\pi_2 = (a, s, \sigma, N)$
- $\pi_3 = (a, s, \sigma, \theta)$

**For  $\pi_1$  - term**

$$\pi_1 = (a^{a_1}, s^{b_1}, \sigma^{c_1}, r)$$

$$M^0 L^0 T^0 = (L)^{a_1} (T^{-1})^{b_1} (ML^{-1}T^{-2})^{c_1} L$$

For M:  $0 = c_1$

For L:  $0 = a_1 - c_1 + 1$

$a_1 = -1$

For T:  $0 = -b_1 - 2c_1$

$$\begin{aligned} 0 &= b_1 \\ \pi_1 &= a^{-1} \cdot s^0 \cdot \sigma^0 \cdot r \\ \pi_1 &= r a^{-1} \end{aligned} \tag{4}$$

**For  $\pi_2$  - term**

$$\pi_2 = (a^{a_2}, s^{b_2}, \sigma^{c_2}, N)$$

$$M^0 L^0 T^0 = (L)^{a_2} (T^{-1})^{b_2} (ML^{-1}T^{-2})^{c_2} L^{-2}$$

For M:  $0 = c_2$

For L:  $0 = a_2 - c_2 - 2$

$a_2 = 2$

For T:  $0 = -b_2 - 2c_2$

$$\begin{aligned} 0 &= b_2 \\ \pi_2 &= a^2 s^0 \sigma^0 N \\ \pi_2 &= a^2 N \end{aligned} \tag{5}$$

**For  $\pi_3$  - term**

$$\pi_3 = (a^{a_3}, s^{b_3}, \sigma^{c_3}, \theta)$$

$$M^0 L^0 T^0 = (L)^{a_3} (T^{-1})^{b_3} (ML^{-1}T^{-2})^{c_3} M^0 L^0 T^0$$

For M:  $0 = c_3$

For L:  $0 = a_3 - 2c_3 - 0$

$a_3 = 2$

For T:  $0 = -b_3 - 2c_3$

$$\begin{aligned} 0 &= b_3 \\ \pi_3 &= a^2 s^0 \sigma^0 \theta \\ \pi_3 &= \theta \end{aligned} \tag{6}$$

From (3), thus,

$$f_1(r a^{-1}, a^2 N, \theta) = 0$$

$$\frac{r}{a} = \phi(a^2 N \theta)$$

$$r = a \phi(a^2 N, \theta) \tag{7}$$

Now deriving the formula for the radius, we can simply have

$$r = a \phi(a^2 N \theta) \tag{8}$$

Equation (9) shows that the ratios between the variables are such that we have

$$a^3 : N : \theta$$

This can be rewritten as;

$$r = \phi[a^3 \sqrt{N^3 \theta}] \tag{10}$$

Equation (10) is the model being derived and used to determine the result for the plastic region size. In the expression,  $r$  = plastic zone size,  $\phi$  = material parameter,  $a$  = crack length,  $\theta$  = crack angle,  $N$  = material property (dislocation density) which is assumed to be  $10^{12} \text{ mm}^{-1}$ .

**B. Experimental Procedure**

Mild steel rods used for this research were obtained from Universal Steel Company, Ogba, Ikeja, Nigeria with composition shown in Table I. The steel rods were machined into a ‘dog bone’ shape for tensile experiment as shown in Fig. 1. The depth varied was 2mm and 4mm, the crack angles used were 45°, 50°, 60°, 70° and 90°. Mechanical test was conducted at five strain rates using a Universal Tensile Testing Machine (Instrong Universal Tensile Testing Machine of model 3369 with a maximum capacity of 50KN shown in Fig. 2) in ambient temperature. Ultimate tensile strength, tensile strain, Modulus of Elasticity, Stress at fracture, Strain at fracture, Yield stress and Yield strain were determined from the tensile test results.

TABLE I  
CHEMICAL COMPOSITION OF PLAIN CARBON STEEL

Element	% Composition
C	0.0355
Si	0.0240
Mn	0.1535
S	0.0230
P	0.0135
Cr	0.0150
Cu	0.0400
Fe	99.651
Ni	0.0170
Others	0.0275

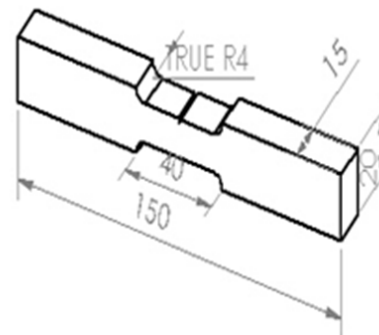


Fig. 1 Three Dimensional diagram of the specimen



Fig. 2 A model 3369 Instron Universal Tensile Testing Machine

Calculation of experimental plastic zone size was done with

$$K_I = \alpha \sigma_f \sqrt{\pi(a+r)} = \alpha \sigma_f \sqrt{\pi a_e} \quad (11)$$

$$r = \frac{1}{2\pi} \left( \frac{K_I}{\sigma_{ys}} \right)^2 \left[ \cos \frac{\theta}{2} (1 + \sin \frac{\theta}{2}) \right] \quad (12)$$

where  $a$  is the crack length,  $\alpha$  is the geometric correction factor,  $\sigma_f$  is the fracture stress deduced from the stress strain curve,  $\sigma_{ys}$  is the yield strength deduced from the stress strain curve and  $\theta$  the crack angle.

### C. Micro Structural Examination

Fractured metal samples were prepared for metallographic examination. The samples were ground and polished to achieve a mirror like surface for proper metallographic analysis. Dilute Hydrochloric acid was used as etchant and the samples were each etched for about two minutes. The surfaces of the samples were viewed and picture taken using the digital metallurgical microscope.

## III. RESULT/DISCUSSION

### A. Calculated Plastic Zone Size from Model

Fig. 3 shows the variation of simulated plastic zone with crack angle for 2mm and 4mm crack depth of the mild steel material. The size of the plastic region is found to vary linearly with crack angle.

### B. Experimental Results

The effect of strain rates on the Ultimate tensile strength of notched mild steel with 2mm depth at various angles are presented in Fig. 4. Samples with 45 degree edge crack shows a steady increase in UTS to a maximum at  $1.9 \times 10^{-3} \text{ s}^{-1}$  (285 MPa) before decreasing. This behavior is also exhibited by samples with 60° and 90° edge cracks. Samples with 50° and 70° degree edge cracks seem to have a fluctuating trend in their UTS. Reference [12] while working on medium carbon steel observed that at a particular strain rate, ultimate tensile strength will increase as the crack angle increases. Crack angles 45°, 60° and 90° all tend to follow similar trend within the range of strain rates to which they were examined with 45° crack angle showing the highest trend in similar to results of

[12]. Crack angle 50° shows the most irregular dependence on strain rate but it shows highest strength of 309.62 MPa at strain rate  $1.43 \times 10^{-3} \text{ s}^{-1}$ . On the average, strain rate  $1.43 \times 10^{-3} \text{ s}^{-1}$  gives the highest UTS (309.62 MPa) whereas the least (230.99 MPa) is shown by  $0.48 \times 10^{-3} \text{ s}^{-1}$ .

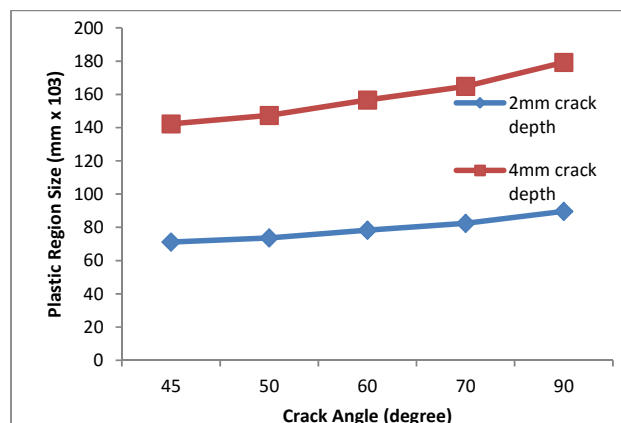


Fig. 3 Plastic zone size and Crack angle

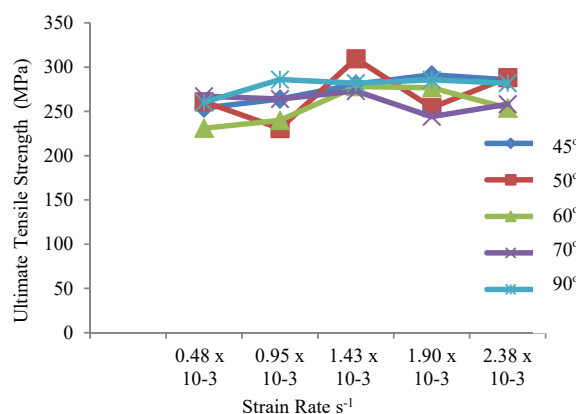


Fig. 4 Ultimate Tensile strength and Strain rate for 2mm Crack depth

The effect of strain rates on the Ultimate tensile strength of notched mild steel with 4mm crack depth at various angles are presented in Fig. 5. Samples with 45° edge crack shows a sharp increase in UTS to a maximum at  $0.95 \times 10^{-3} \text{ s}^{-1}$  (291.22 MPa) strain rate and decrease gradually with increase in strain rate. This behavior is also exhibited by samples with 90° edge cracks. Samples with 50° edge cracks experience gradual increase in UTS to a maximum at  $1.9 \times 10^{-3} \text{ s}^{-1}$  (259 MPa) and decreases afterwards with increase in strain rate. Samples with 60° edge crack show a steady increase in UTS to a maximum at  $2.38 \times 10^{-3} \text{ s}^{-1}$  whereas those of 70° and 90° decreases steadily throughout the range of the test. The highest UTS is shown by 45° cracked sample (291.62) MPa at strain rate  $0.95 \times 10^{-3} \text{ s}^{-1}$  consistent with the result obtained from 2mm crack depth, whereas the least (193 MPa) is shown by 90° at  $0.48 \times 10^{-3} \text{ s}^{-1}$  strain rate.

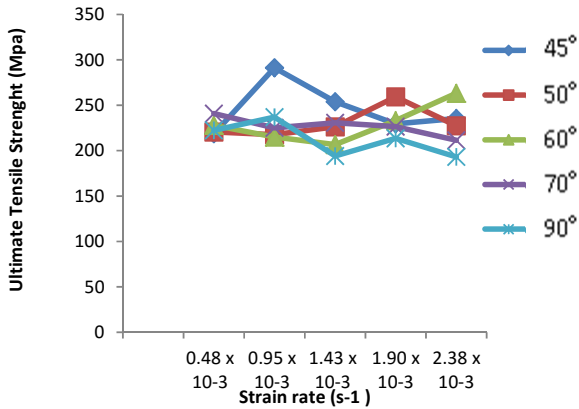


Fig. 5 Ultimate Tensile Strength and Strain rate for 4mm Crack depth

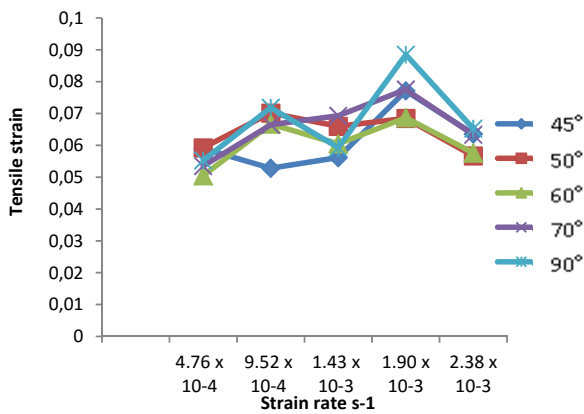


Fig. 6 Strain at maximum load and Strain rate for 2mm Crack depth

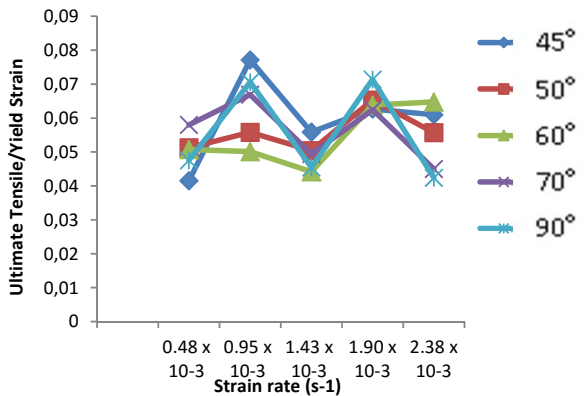


Fig. 7 Strain at maximum load and Strain rate for 4mm Crack depth

The variation of strain at maximum load of samples with strain rate and crack angle is shown in Figs. 6 and 7. The figures shows strain to be highest (0.089) in 90° crack angle specimen for 2mm crack depth and 0.077 for crack angle 45° in 4mm crack depth. These results show the dependence of ductility on crack depth. Ductility decreases as the crack depth increases for a particular crack angle and at a particular strain rate. In Fig. 6 at  $1.9 \times 10^{-3} \text{ s}^{-1}$ , the highest ductility (0.089) was

obtained similar to that in Fig. 7. Increase in ductility as the strain rate increases occurs only at crack angles 45° and 70° between  $0.95 \times 10^{-3} \text{ s}^{-1} - 1.90 \times 10^{-3} \text{ s}^{-1}$  and  $0.48 \times 10^{-3} \text{ s}^{-1} - 1.90 \times 10^{-3} \text{ s}^{-1}$  respectively in Fig. 6 while Fig. 7 does not really show such clear cut pattern.

The effect of strain rate and crack angle on the fracture stress of samples is shown in Figs. 8 and 9. Results show that the highest fracture stress (220.92 MPa) is shown by 90° crack angle at a strain rate of  $0.95 \times 10^{-3} \text{ s}^{-1}$  and least (20.01 MPa) at  $2.38 \times 10^{-3} \text{ s}^{-1}$ . Crack angle 45° show low values of fracture stresses in the both conditions at the same strain rate of  $0.48 \times 10^{-3} \text{ s}^{-1}$  and  $2.38 \times 10^{-3} \text{ s}^{-1}$ . Crack angle 50° maintains a high value of fracture stress at 2mm depth. These results show that the fracture stress is dependent on the crack depth and angle. This is consistent with the findings of [12] that under loading, critical stress at which a material will break or fracture will be a function of crack depth and strain rate. Moreover it was also observed that for a particular strain rate, the fracture load will increase as the crack angle increases and decrease as the depth increases.

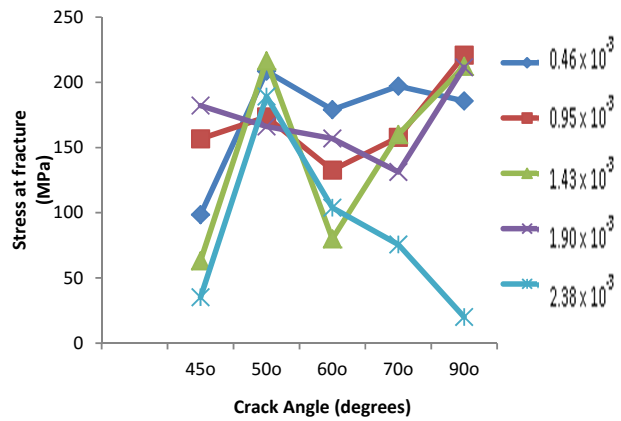


Fig. 8 Stress at Fracture and Crack Angle for 2mm Crack depth

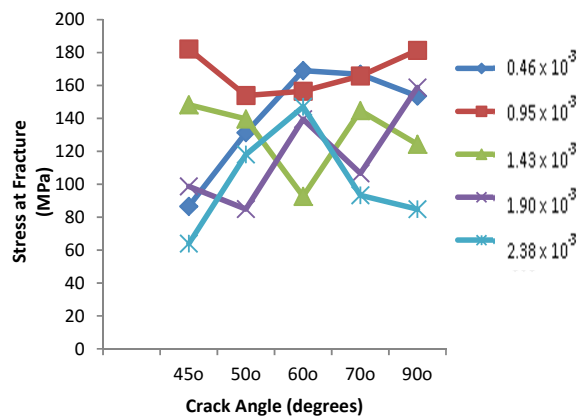


Fig. 9 Stress at Fracture and Crack Angle for 4mm Crack depth

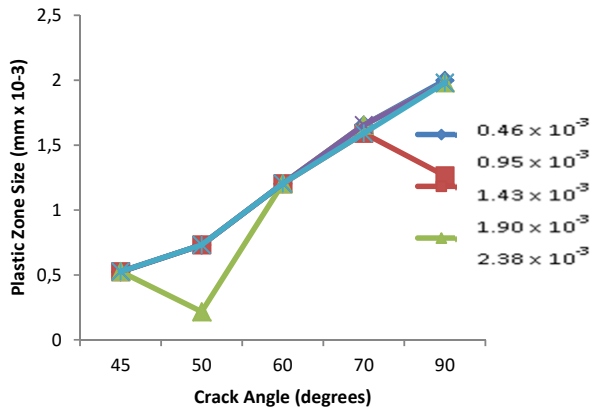


Fig. 10 Plastic zone size using Tresca's yield for 2mm crack depth

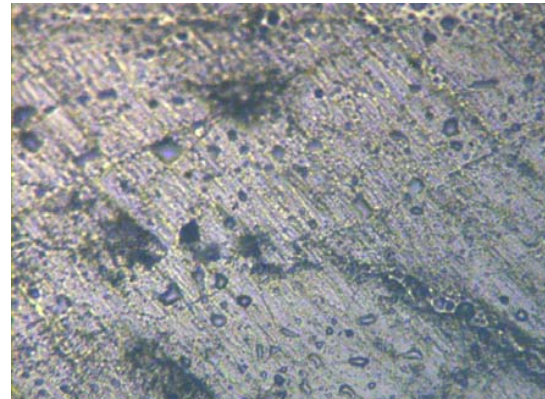


Fig. 12 Plastic zone size of specimen with crack depth of 2mm at crack angle of 50° that was fractured at strain rate  $0.48 \times 10^{-3} \text{ s}^{-1}$

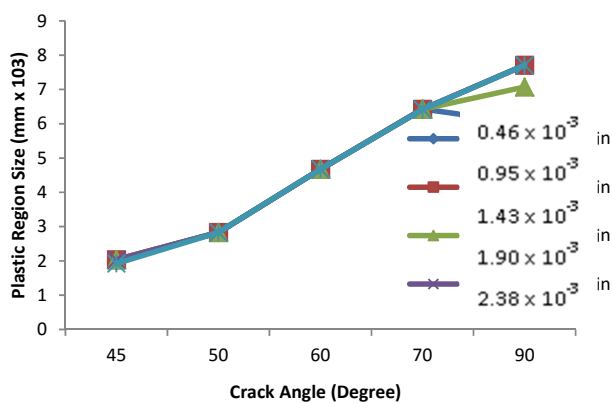


Fig. 11 Plastic zone size using Tresca's yield criterion for 4mm crack depth

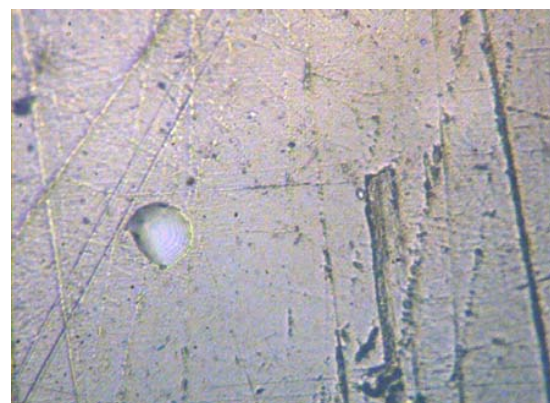


Fig. 13 Plastic zone size of specimen with crack depth of 2mm at crack angle of 50° that was fractured at strain rate  $1.43 \times 10^{-3} \text{ s}^{-1}$

Figs. 10 and 11 show the variation of plastic region size of Single Edge Notched specimens subjected to varying strain rates with crack angle. The plastic zone sizes have same values in specimens with same crack angles irrespective of the strain rate. This shows that the plastic zone size is not affected by the difference in strain rate. Increase in crack angle led to a steady increase in plastic zone size. Some deviations are seen at some instances which may be attributed to the presence of inclusion sites scattered over the matrix surface of the affected samples which may have caused dislocation pile ups and stress concentration points as observed in the micrographs of the affected samples (see Figs. 12-14, 16 and 17) These might suggest that inclusions have the tendency of reducing the plastic zone size. The texture observed in Fig. 15 depicts that the material has higher strength than the material having the microstructure in Fig. 14, thus there is more resistance to deformation in material having the microstructure of Fig. 15 than microstructure of Fig. 14. Moreover, presence of more voids in material having microstructure of Fig. 14 depicts that dislocation moves with more ease than material having microstructure of Fig. 15. Therefore, plastic zone sizes will be smaller in high strength materials when compared to low strength materials.

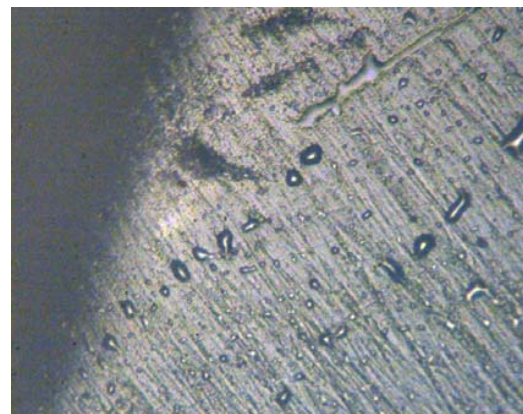


Fig. 14 Plastic region of specimen with crack depth of 2mm at crack angle of 90° that was fractured at strain rate  $0.46 \times 10^{-3} \text{ s}^{-1}$





Fig. 15 Plastic region of specimen with crack depth of 2mm at crack angle of 90° that was fractured at strain rate  $0.95 \times 10^{-3} \text{ s}^{-1}$

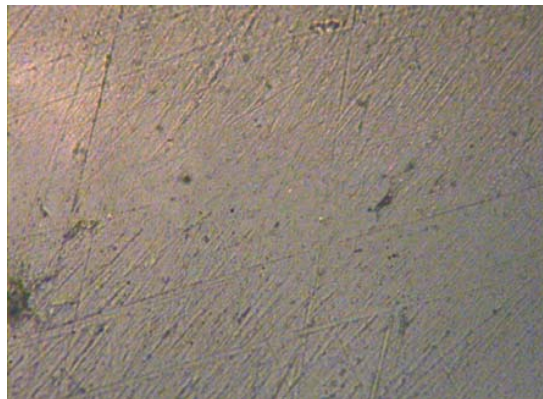


Fig. 18 Specimen with crack angle of 90° with crack depth of 4mm that was fractured at strain rate  $0.48 \times 10^{-3} \text{ s}^{-1}$

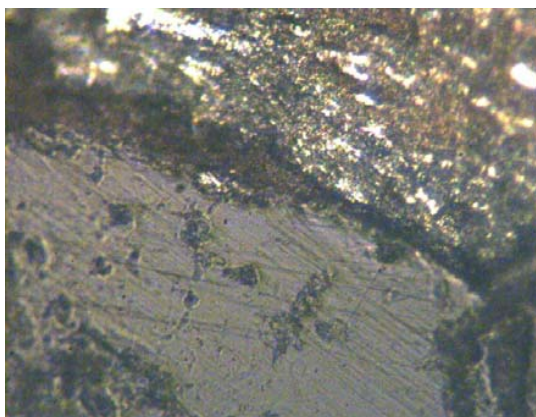


Fig. 16 Specimen with crack angle of 90° with crack depth of 4mm that was fractured at strain rate  $2.38 \times 10^{-3} \text{ s}^{-1}$



Fig. 17 Specimen with crack angle of 90° with crack depth of 4mm that was fractured at strain rate  $1.43 \times 10^{-3} \text{ s}^{-1}$

#### IV. CONCLUSION

This study has shown that

1. Plastic zone size can be expressed in terms of crack parameters (crack size and crack angle) and material property while avoiding parameters that would require sophisticated equipment to determine.
2. Plastic zone size for low carbon steel increases as the crack angle increases while it is independent of strain rate for a particular crack angle.
3. The low presence of inclusions and fine textures are suggested to cause lower plastic zone sizes in the affected specimens.
4. The numerical tool used in deriving the model shows that the plastic zone size can be derived without the use of complex analytical or numerical method..

#### REFERENCES

- [1] K.J. Kang, H.G. Beom, "Plastic zone size near the crack tip in a constrained ductile layer under mixed mode loading", Engineering Fracture Mechanics vol 66, pp 257 – 268, 2000.
- [2] A. Tanaka and T. Yamauchi "Size Estimation of Plastic Deformation Zone at the Crack Tip of Paper under Fracture Toughness Testing", J. Pack. Science and Technology, vol.6, no.5, pp 268 -275, 1997.
- [3] N.Perez. Fracture Mechanics, Kluwer Academic Publisher, pp 95-112, 2004.
- [4] Y.J Kim, G. Lin, A. Cornec, W. Brocks, K.H. Schwalbe. "The Maximum Stresses in the Constrained Ductile Layer under Smallscale Yielding Conditions", Int. Journal of Fracture, vol 75, pp 9 – 16, 1996.
- [5] Hill R. In: *Mathematical theory of plasticity*. Oxford: Oxford University Press, pp 226 – 256, 1950.
- [6] E.S Foliass. "Estimating Plastic Zone Size" International Journal of fracture, vol 10 no1, pp 109 – 111, 1974.
- [7] D.K Choi and J.Kim, "A study on distribution of plastic region near a crack tip using three-dimensional molecular dynamics simulation," Journals of Metals and Materials, vol. 4, No. 4, pp 925, 1998.
- [8] M.T Welsch, M. Henning, M.Marx and H. Vehoff, "Measuring the Plastic Zone Size by Orientation Gradient Mapping (OGM) and Electron Channeling Contrast Imaging (ECCI)". Adv. Eng. Material, vol 9, pp 31–37, 2007.
- [9] www.maplesoft.com/engineering/mechanical/monotonic plasticzonesize
- [10] G.R. Irwin. "Plastic zone near a crack and fracture toughness". In: Proceedings of 7th Sagamore Conference. Pp 4 – 63, 1960.
- [11] D.S. Dugdale. Yielding in steel sheet containing slits. Journal of Mech Phys Solids; vol 8, pp 100 - 104, 1960.
- [12] S. K. Nath, K. D. Uttam. *Effect of Microstructure and Notches on the Fracture Toughness of Medium Carbon Steel*. Journal of Naval Architecture and Marine Engineering, pp 15-22, 2006.